

Effect of inelastic scattering on the nuclear magnetic relaxation rate $1/T_1T$ in iron-based superconductors

Youichi YAMAKAWA,¹ Seiichiro ONARI,² and Hiroshi KONTANI¹

¹*Department of Physics, Nagoya University and JST, TRIP, Furo-cho, Nagoya 464-8602, Japan.*

²*Department of Applied Physics, Nagoya University and JST, TRIP, Furo-cho, Nagoya 464-8603, Japan.*

(Dated: June 20, 2018)

We present a microscopic study of the nuclear magnetic relaxation rate $1/T_1$ based on the five-orbital model for iron-based superconductors. We mainly discuss the effect of the “inelastic” quasi-particle damping rate γ due to many-body interaction on the size of the coherence peak, for both s_{++} and s_{\pm} -wave superconducting states. We focus on $\text{Ba}(\text{Fe}_{1-x}\text{Co}_x)_2\text{As}_2$, and systematically evaluate γ in the normal state from the experimental resistivity, from optimally to over-doped compounds. Next, γ in the superconducting state is calculated microscopically based on the second order perturbation theory. In optimally doped compounds ($T_c \sim 30$ K), it is revealed that the coherence peak on $1/T_1T$ is completely suppressed due to large γ for both s_{++} and s_{\pm} -wave states. On the other hand, in heavily over doped compounds with $T_c < 10$ K, the coherence peak could appear for both pairing states, since γ at T_c is quickly suppressed in proportion to T_c^2 . By making careful comparison between theoretical and experimental results, we conclude that it is difficult to discriminate between s_{++} and s_{\pm} -wave states from the present experimental results.

I. INTRODUCTION

Since the discovery of superconductivity in $\text{LaFeAsO}_{1-x}\text{F}_x$,¹ the superconducting mechanism and pairing symmetry had been discussed intensively. In many optimally-doped compounds, the superconducting gap is fully gapped as reported by the penetration depth measurement² and the angle-resolved photoemission spectroscopy (ARPES).^{3,4} As for the superconducting mechanism, the s -wave pairing with sign change of the order parameter between the hole and electron Fermi pockets, so called s_{\pm} -wave, mediated by the anti-ferromagnetic fluctuation had been proposed from the early stage as a possible pairing state in the iron pnictides.⁵⁻⁹ It is supported by quasi-particle interference analysis by Scanning Tunneling Microscopy/Spectroscopy (STM/STS) measurement by Hanaguri *et al.*¹⁰ However, the small T_c -suppression against nonmagnetic impurities is not consistent with the s_{\pm} -wave state.¹¹⁻¹⁵

On the other hand, orbital fluctuation mediated s -wave superconducting state without sign reversal (s_{++} -wave state) had been investigated.¹⁶ We have shown that strong ferro- and antiferro-orbital fluctuations develop due to the combination of Coulomb and e -ph interactions.¹⁷⁻²¹ Consistently, large softening of the shear modulus C_{66} ²²⁻²⁴ and renormalization of phonon velocity²⁵ are observed well above the orthorhombic structure transition temperature T_s . These phenomena strongly suggest the existence of strong ferro-orbital (charge quadrupole $O_{x^2-y^2}$) fluctuations, considering the large strain-quadrupole coupling.¹⁹⁻²¹ In addition, experimental “resonance-like” hump structure in the neutron inelastic scattering is well reproduced in terms of the s_{++} -wave state.^{26,27}

The nuclear-magnetic resonance (NMR) and the nuclear-quadrupole resonance (NQR) measurements are

useful for the discussion of the pairing symmetry. The coherence effect of superconductivity, appearing as a Hebel-Slichter peak (coherence peak) in the nuclear spin relaxation rate ($1/T_1$), was one of the crucial experimental proofs of the Bardeen-Cooper-Schrieffer (BCS) theory, characterized by conventional s -wave Cooper pairs with an isotropic gap.²⁸ In the Fe based superconductors, many experimental results of $1/T_1$ have been published.²⁹⁻³⁵ It was found that the coherence peak in $1/T_1$ is absent in many compounds, like electron-doped $\text{Ba}(\text{Fe}_{1-x}\text{Co}_x)_2\text{As}_2$ and hole-doped $\text{Ba}_{1-x}\text{K}_x\text{Fe}_2\text{As}_2$.

The size of the coherence peak had attracted great attention to distinguish between s_{++} and s_{\pm} -wave states: In a simple BCS theory, the peak size is larger in the s_{++} -wave state, while it is reduced in the s_{\pm} -wave state. However, the coherence peak is suppressed by the “inelastic” quasi-particle damping rate γ , which is prominent in moderately and strongly correlated systems.^{36,37} For this reason, the coherence peak is not observed even in several conventional s -wave superconductors with $T_c > 15$ K, such as boron carbide $\text{YNi}_2\text{B}_2\text{C}$ ³⁸ and A-15 compounds V_3Si .³⁹ Thus, inelastic scattering due to many-body effect has to be taken into account for a quantitative analysis of $1/T_1$.

Impurity effect (=“elastic” quasi-particle damping effect) on T_c and $1/T_1$ is also important in studying the pairing symmetry. In the s_{++} -wave state, both T_c and $1/T_1$ are insensitive to impurities. In contrast, the s_{\pm} -wave state is easily suppressed by impurities like the d -wave state, according to the study based on the five-orbital model.¹⁵ The impurity-induced gapless state in the s_{\pm} -wave state would give strong influence on $1/T_1$ for $T \ll T_c$.^{7,40,41} However, impurity-induced gapless state is realized only when T_c is strongly suppressed to be $\sim T_{c0}/3$ theoretically.⁴² Thus, gapless behavior of $1/T_1$ for $T \ll T_c$ observed in some compounds cannot be explained by this scenario.

Recently, authors in Refs. 43 and 44 had shown

that the coherence peak in the s_{++} -wave state disappears when inelastic scattering γ at T_c is as large as the superconducting gap at $T = 0$. However, quantitative estimations of γ and its T and ω dependences are still lacking. Interestingly, recent NMR measurement reports a small coherence peak of $1/T_1$ in the heavily over doped $\text{LaFeAsO}_{1-x}\text{F}_x$ with low transition temperature $T_c \sim 5$ K.³⁵ Now, microscopic study of $1/T_1$ by including inelastic scattering effect is desired to discuss the superconducting pairing state as s_{\pm} or s_{++} .

In this paper, we investigate the effect of inelastic scattering rate γ on the nuclear magnetic relaxation rate $1/T_1$ for both s_{++} and s_{\pm} -wave states. For a quantitative discussion on the existence of the Hebel-Slichter coherence peak, we employ the two-dimensional five orbital model.⁵ Here, γ is the key parameter of the present study: At T_c , the value of γ is carefully estimated from the experimental conductivity,²⁷ and its temperature and the frequency dependences below T_c is obtained by the second order perturbation theory. All results shown below are obtained with band filling $n = 6.1$.

The contents of this paper are as follows; In Sec. II, we explain how to calculate the nuclear magnetic relaxation rate $1/T_1T$ and quasi-particle damping γ . The obtained numerical results are explained in Sec. III. Finally, we make comparison between theoretical and experimental results in Sec. IV, and discuss the possible pairing symmetry.

II. FORMULATION

A. Green function

Now, we study the 10×10 Nambu BCS Hamiltonian $\hat{\mathcal{H}}_{\mathbf{k}}$ composed of the five orbital tight binding model⁵ and the band-diagonal SC gap.¹⁵ The Hamiltonian is given by

$$\hat{\mathcal{H}}^0 = \sum_{\mathbf{k}} \hat{c}_{\mathbf{k}}^{\dagger} \hat{\mathcal{H}}_{\mathbf{k}}^0 \hat{c}_{\mathbf{k}}, \quad (1)$$

where $\hat{c}_{\mathbf{k}}^{\dagger}$ and $\hat{c}_{\mathbf{k}}$ are vectors,

$$\hat{c}_{\mathbf{k}}^{\dagger} = \left(c_{1,\mathbf{k},\uparrow}^{\dagger}, \dots, c_{5,\mathbf{k},\uparrow}^{\dagger}, c_{1,-\mathbf{k},\downarrow}, \dots, c_{5,-\mathbf{k},\downarrow} \right), \quad (2)$$

and $c_{\alpha,\mathbf{k},\sigma}^{\dagger}$ ($c_{\alpha,\mathbf{k},\sigma}$) is a creation (annihilation) operator of an electron for band α with wave vector \mathbf{k} and spin σ . $\hat{\mathcal{H}}_{\mathbf{k}}^0$ is 10×10 Nambu BCS Hamiltonian given as

$$\hat{\mathcal{H}}_{\mathbf{k}}^0 = \begin{pmatrix} \hat{H}_{\mathbf{k}} & \hat{\Delta}_{\mathbf{k}} \\ \hat{\Delta}_{\mathbf{k}}^{\dagger} & -\hat{H}_{\mathbf{k}} \end{pmatrix}, \quad (3)$$

where $\hat{H}_{\mathbf{k}}$ and $\hat{\Delta}_{\mathbf{k}}$ are 5×5 matrices in the band-diagonal basis,

$$\hat{H}_{\mathbf{k}} = \begin{pmatrix} \epsilon_{1,\mathbf{k}} & & & & 0 \\ & \ddots & & & \\ 0 & & & & \epsilon_{5,\mathbf{k}} \end{pmatrix}, \quad \hat{\Delta}_{\mathbf{k}} = \begin{pmatrix} \Delta_{1,\mathbf{k}} & & & & 0 \\ & \ddots & & & \\ 0 & & & & \Delta_{5,\mathbf{k}} \end{pmatrix} \quad (4)$$

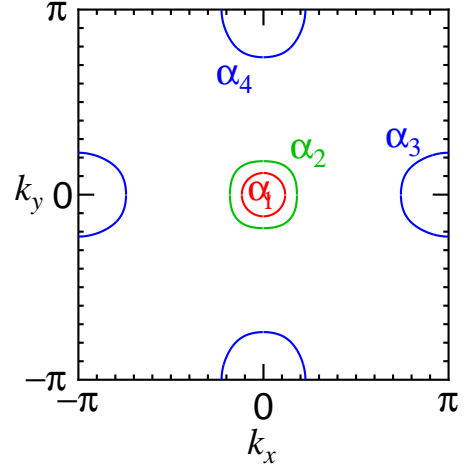


FIG. 1. Fermi surfaces of the 5 bands model for iron pnictide in the unfolded Brillouin zone.

where $\epsilon_{\alpha,\mathbf{k}}$ and $\Delta_{\alpha,\mathbf{k}}$ are a dispersion and a gap function of quasi particle for α and \mathbf{k} , respectively. Figure 1 shows the Fermi surface (1 Fe atom/unit cell) for electron doped iron pnictides. Fermi surface α_1 and α_2 around Γ point are hole pockets and α_3 and α_4 are electron pockets. Hereafter, we approximate $\Delta_{\alpha,\mathbf{k}}$ as follows:

$$\Delta_{\alpha,\mathbf{k}} \approx \Delta_{\alpha} = \Delta_{\alpha}^0 \tanh \left(\frac{\pi}{2} \sqrt{\frac{T_c}{T} - 1} \right), \quad (5)$$

where Δ_{α}^0 is a superconducting gap at zero temperature and, in the present work, we assume that the superconducting gaps for each band are \mathbf{k} -independent.

The 10×10 Green's function $\hat{\mathcal{G}}_{\mathbf{k}}$ in the Nambu representation is given by⁴⁵

$$\hat{\mathcal{G}}_{\mathbf{k}}(i\omega_n) = \left(i\omega_n \hat{1} - \hat{\mathcal{H}}_{\mathbf{k}}^0 - \hat{\Sigma}_{\mathbf{k}}(i\omega_n) \right)^{-1}, \quad (6)$$

where $\omega_n = \pi T(2n + 1)$ is the fermion Matsubara frequency. The normal self energy $\hat{\Sigma}_{\mathbf{k}}(i\omega_n)$ represents the inelastic quasi-particle damping and mass enhancement due to many-body interactions. We neglect the impurity induced self energy since it does not change the density of states (DOS) in a simple s -wave state, Eq. (5) (Anderson theorem). When $\hat{\Sigma}_{\mathbf{k}}(i\omega_n)$ has band diagonal form, Eq. (6) also becomes a band diagonal form, and the Green's function for band α is given by a 2×2 matrix,

$$\begin{aligned} \hat{\mathcal{G}}_{\alpha,\mathbf{k}}(i\omega_n) &= \begin{pmatrix} i\omega_n - \epsilon_{\alpha,\mathbf{k}} - \Sigma_{\alpha,\mathbf{k}}(i\omega_n) & -\Delta_{\alpha} \\ -\Delta_{\alpha} & i\omega_n + \epsilon_{\alpha,\mathbf{k}} + \Sigma_{\alpha,\mathbf{k}}(-i\omega_n) \end{pmatrix}^{-1} \\ &= \frac{1}{|\hat{\mathcal{G}}_{\alpha,\mathbf{k}}(i\omega_n)^{-1}|} \\ &\quad \times \begin{pmatrix} i\omega_n + \epsilon_{\alpha,\mathbf{k}} + \Sigma_{\alpha,\mathbf{k}}(-i\omega_n) & \Delta_{\alpha} \\ \Delta_{\alpha} & i\omega_n - \epsilon_{\alpha,\mathbf{k}} - \Sigma_{\alpha,\mathbf{k}}(i\omega_n) \end{pmatrix} \\ &\equiv \begin{pmatrix} G_{\alpha,\mathbf{k}}(i\omega_n) & F_{\alpha,\mathbf{k}}(i\omega_n) \\ F_{\alpha,\mathbf{k}}(i\omega_n) & -G_{\alpha,\mathbf{k}}(-i\omega_n) \end{pmatrix}, \end{aligned} \quad (7)$$

where $|\hat{\mathcal{G}}_{\alpha,\mathbf{k}}(i\omega_n)^{-1}|$ is the determinant of the inverse matrix of the Green's function, and $G_{\alpha,\mathbf{k}}$, $F_{\alpha,\mathbf{k}}$ and $\Sigma_{\alpha,\mathbf{k}}$ are the normal Green's function, the anomalous Green's function and the normal self-energy for band α with wave vector \mathbf{k} , respectively. The local Green's function $\hat{\mathbf{g}}_{\alpha}$ is obtained by the \mathbf{k} summation;

$$\begin{aligned}\hat{\mathbf{g}}_{\alpha}(i\omega_n) &= \frac{1}{N} \sum_{\mathbf{k}} \hat{\mathcal{G}}_{\alpha,\mathbf{k}}(i\omega_n) \\ &= \int_{-\infty}^{\infty} d\epsilon N(\epsilon) \hat{\mathcal{G}}_{\alpha}(\epsilon, i\omega_n),\end{aligned}\quad (8)$$

where $N(\epsilon)$ is the quasi-particle DOS. In this ϵ integral, the dominant contribution comes from the explicit ϵ term of the denominator $|\hat{\mathcal{G}}_{\alpha,\mathbf{k}}(i\omega_n)^{-1}|$. By neglecting the ϵ dependence of $N(\epsilon)$ and applying the infinite dimensional approximation for $\Sigma_{\alpha}(\epsilon, i\omega_n)$ (see the following subsection II C), we obtain

$$\begin{aligned}\hat{\mathbf{g}}_{\alpha}(i\omega_n) &\approx \frac{-\pi N(0)}{\sqrt{\tilde{\omega}_{\alpha}(i\omega_n)^2 + \Delta_{\alpha}^2}} \begin{pmatrix} i\tilde{\omega}_{\alpha}(i\omega_n) & \Delta_{\alpha} \\ \Delta_{\alpha} & i\tilde{\omega}_{\alpha}(i\omega_n) \end{pmatrix} \\ &\equiv \begin{pmatrix} g_{\alpha}(i\omega_n) & f_{\alpha}(i\omega_n) \\ f_{\alpha}(i\omega_n) & g_{\alpha}(i\omega_n) \end{pmatrix}.\end{aligned}\quad (9)$$

From the five orbital model, the total DOS per spin is $N(0) = 0.66 \text{ eV}^{-1}$ at Fermi level. Then, analytic continuation ($i\omega_n \rightarrow \tilde{\omega} = \omega + i\delta$) yields the retarded Green's function as follows,

$$\begin{aligned}g_{\alpha}^{\text{R}}(\omega) &= \frac{-\pi N(0)\tilde{\omega}_{\alpha}^{\text{R}}(\omega)}{\sqrt{-\tilde{\omega}_{\alpha}^{\text{R}}(\omega)^2 + \Delta_{\alpha}^2}}, \\ f_{\alpha}^{\text{R}}(\omega) &= \frac{-\pi N(0)\Delta_{\alpha}}{\sqrt{-\tilde{\omega}_{\alpha}^{\text{R}}(\omega)^2 + \Delta_{\alpha}^2}},\end{aligned}\quad (10)$$

where $\tilde{\omega}_{\alpha}^{\text{R}}(\omega)$ is defined as

$$\begin{aligned}\tilde{\omega}_{\alpha}^{\text{R}}(\omega) &= \tilde{\omega} - i\text{Im}\Sigma_{\alpha}^{\text{R}}(\omega) \\ &= \tilde{\omega} + i\gamma_{\alpha}^*,\end{aligned}\quad (11)$$

where γ^* is the ‘‘renormalized’’ quasi-particle damping, which is described by using ‘‘unrenormalized’’ quasi-particle damping $\gamma \equiv -\text{Im}\Sigma^{\text{R}}$ and bare and effective masses m and m^* as

$$\gamma^* \equiv \frac{m}{m^*}\gamma.\quad (12)$$

The mass enhancement factor m^*/m is given by

$$\frac{m^*}{m} = 1 - \lim_{\omega \rightarrow 0} \frac{\partial \text{Re}\Sigma^{\text{R}}(\omega)}{\partial \omega},\quad (13)$$

which is reported as $1 \sim 3$ for iron pnictides called 1111 and 122 systems from various experiments such as de Haas-van Alphen measurements,^{46–48} optical spectral weight,⁴⁹ and Seebeck effect with specific heat.⁵⁰ The mass enhancement factor has a relatively large value in the optimally doped systems and gradually decreases by carrier doping.

B. Nuclear Magnetic Relaxation Rate

The nuclear magnetic relaxation rate $1/T_1T$ in the superconducting state is given by the standard formula:

$$\frac{1}{T_1T} \propto \frac{1}{N} \sum_{\alpha,\mathbf{q}} \lim_{\omega \rightarrow 0} \text{Im} \frac{\chi_{\alpha,\mathbf{q}}^{\text{R}}(\omega)}{\omega},\quad (14)$$

where $\chi_{\mathbf{q}}^{\text{R}}(\omega)$ is the superconducting spin susceptibility and given by

$$\begin{aligned}\text{Im}\chi_{\alpha,\mathbf{q}}^{\text{R}}(\omega) &= \frac{1}{2\pi N} \sum_{\beta,\mathbf{k}} \int_{-\infty}^{\infty} d\omega' \left(\tanh \frac{\omega + \omega'}{2T} - \tanh \frac{\omega'}{2T} \right) \\ &\times \left(\text{Im}G_{\beta,\mathbf{k}+\mathbf{q}}^{\text{R}}(\omega + \omega') \text{Im}G_{\alpha,\mathbf{k}}^{\text{R}}(\omega') \right. \\ &\quad \left. + \text{Im}F_{\beta,\mathbf{k}+\mathbf{q}}^{\text{R}}(\omega + \omega') \text{Im}F_{\alpha,\mathbf{k}}^{\text{R}}(\omega') \right).\end{aligned}\quad (15)$$

In Eq. (14), the limitation becomes a differential of hyperbolic tangent and each summation of α , β , \mathbf{k} and \mathbf{q} can be calculated independently. Then, $1/T_1T$ becomes

$$\begin{aligned}\frac{1}{T_1T} &\propto \int_{-\infty}^{\infty} d\omega \frac{\text{Im}g^{\text{R}}(\omega)^2 + \text{Im}f^{\text{R}}(\omega)^2}{4\pi T \cosh^2(\omega/2T)} \\ &\equiv \int_{-\infty}^{\infty} d\omega X(\omega),\end{aligned}\quad (16)$$

with

$$\begin{aligned}g^{\text{R}}(\omega) &\equiv \sum_{\alpha} g_{\alpha}^{\text{R}}(\omega), \\ f^{\text{R}}(\omega) &\equiv \sum_{\alpha} f_{\alpha}^{\text{R}}(\omega),\end{aligned}\quad (17)$$

where the integrand of ω was defined as $X(\omega)$.

C. Second order perturbation theory

A quasi-particle excitation is well defined if the damping rate γ is small compared to the energy scale. In this case, the quasi-particle damping rate γ can generally be computed from the imaginary part of the normal self energy,⁵¹

$$\text{Im}\Sigma_{\mathbf{k}}^{\text{R}}(\omega) = -\gamma_{\mathbf{k}}(\omega).\quad (18)$$

By using the second order perturbation theory, we derive the microscopic picture of γ and analyze the NMR experimental result. We calculate the electron-electron scattering based on the single band Hubbard model for simplicity. From the second order perturbation theory, the self energy $\Sigma_{\mathbf{k}}$ due to the electron-electron scattering is given by

$$\Sigma_{\mathbf{k}}(i\omega_n) = \frac{V_{\text{eff}}^2 T}{N} \sum_{\mathbf{k}',n'} G_{\mathbf{k}'}^0(i\omega_{n'}) \chi_{\mathbf{k}-\mathbf{k}'}^0(i\omega_n - i\omega_{n'})\quad (19)$$

where V_{eff} is the effective electron-electron interaction enhanced by spin and orbital fluctuations. Its value can

be estimated from the observed conductivity in subsection II D. The imaginary part of the retarded self energy, which is obtained by the analytic continuation, is given by,

$$\begin{aligned} \text{Im}\Sigma_{\mathbf{k}}^{\text{R}}(\omega) &= \frac{V_{\text{eff}}^2}{2\pi N} \sum_{\mathbf{k}'} \int_{-\infty}^{\infty} d\omega' \left(\tanh \frac{\omega'}{2T} + \coth \frac{\omega - \omega'}{2T} \right) \\ &\quad \times \text{Im}G_{\mathbf{k}'}^{0,\text{R}}(\omega') \text{Im}\chi_{\mathbf{k}-\mathbf{k}'}^{0,\text{R}}(\omega - \omega'), \end{aligned} \quad (20)$$

where the superscript “0” on the Green function and susceptibility means the absence of self-energy correction.

In the infinite dimensional approximation, the each summation of wave vectors can be taken independently and we obtain the quasi-particle damping rate due to the

electron-electron scattering as,

$$\begin{aligned} \gamma(\omega) &\equiv \frac{1}{N} \sum_{\mathbf{k}} \gamma_{\mathbf{k}}(\omega) = -\frac{1}{N} \sum_{\mathbf{k}} \text{Im}\Sigma_{\mathbf{k}}(\omega) \\ &= -\frac{V_{\text{eff}}^2}{2\pi} \int_{-\infty}^{\infty} d\omega' \left(\tanh \frac{\omega'}{2T} + \coth \frac{\omega - \omega'}{2T} \right) \\ &\quad \times \text{Im}g^{0,\text{R}}(\omega') \text{Im}\chi^{0,\text{R}}(\omega - \omega'), \end{aligned} \quad (21)$$

with bare susceptibility,

$$\begin{aligned} \text{Im}\chi^{0,\text{R}}(\omega) &= \frac{1}{2\pi} \int_{-\infty}^{\infty} d\omega' \left(\tanh \frac{\omega + \omega'}{2T} - \tanh \frac{\omega'}{2T} \right) \\ &\quad \times (\text{Im}g^{0,\text{R}}(\omega + \omega') \text{Im}g^{0,\text{R}}(\omega')) \\ &\quad + \text{Im}f^{0,\text{R}}(\omega + \omega') \text{Im}f^{0,\text{R}}(\omega'). \end{aligned} \quad (22)$$

To see the role of coherence factor, we rewrite the imaginary part of the Green’s functions with $\text{Im}G_{\mathbf{k}}^{0,\text{R}}(\omega) = -\frac{\pi}{2} \left\{ \left(1 + \frac{\epsilon_{\mathbf{k}}}{E_{\mathbf{k}}}\right) \delta(\omega - E_{\mathbf{k}}) + \left(1 - \frac{\epsilon_{\mathbf{k}}}{E_{\mathbf{k}}}\right) \delta(\omega + E_{\mathbf{k}}) \right\}$ and $\text{Im}F_{\mathbf{k}}^{0,\text{R}}(\omega) = -\frac{\pi\Delta_{\mathbf{k}}}{2E_{\mathbf{k}}} \left\{ \delta(\omega - E_{\mathbf{k}}) - \delta(\omega + E_{\mathbf{k}}) \right\}$, where $E_{\mathbf{k}} \equiv \sqrt{\epsilon_{\mathbf{k}}^2 + \Delta_{\mathbf{k}}^2}$. By neglecting the energy-dependence of the DOS near the Fermi level, we obtain another notation of the self energy as,

$$\begin{aligned} \text{Im}\Sigma_{\mathbf{k}}^{\text{R}}(\omega) &= -\frac{\pi V_{\text{eff}}^2}{4N^2} \sum_{\mathbf{k}'} \sum_{\mathbf{k}''} \frac{\cosh \frac{\omega}{2T}}{\cosh \frac{E_{\mathbf{k}'}}{2T} \cosh \frac{E_{\mathbf{k}-\mathbf{k}'+\mathbf{k}''}}{2T} \cosh \frac{E_{\mathbf{k}''}}{2T}} \\ &\quad \times \frac{1}{8} \left[\left(1 + \frac{\Delta_{\mathbf{k}-\mathbf{k}'+\mathbf{k}''} \Delta_{\mathbf{k}''}}{E_{\mathbf{k}-\mathbf{k}'+\mathbf{k}''} E_{\mathbf{k}''}}\right) \left\{ \delta(|\omega| - |E_{\mathbf{k}'} + E_{\mathbf{k}-\mathbf{k}'+\mathbf{k}''} - E_{\mathbf{k}''}|) + \delta(|\omega| - |E_{\mathbf{k}'} - E_{\mathbf{k}-\mathbf{k}'+\mathbf{k}''} + E_{\mathbf{k}''}|) \right\} \right. \\ &\quad \left. + \left(1 - \frac{\Delta_{\mathbf{k}-\mathbf{k}'+\mathbf{k}''} \Delta_{\mathbf{k}''}}{E_{\mathbf{k}-\mathbf{k}'+\mathbf{k}''} E_{\mathbf{k}''}}\right) \left\{ \delta(|\omega| - |E_{\mathbf{k}'} - E_{\mathbf{k}-\mathbf{k}'+\mathbf{k}''} - E_{\mathbf{k}''}|) + \delta(|\omega| - |E_{\mathbf{k}'} + E_{\mathbf{k}-\mathbf{k}'+\mathbf{k}''} + E_{\mathbf{k}''}|) \right\} \right] \end{aligned} \quad (23)$$

For $T \lesssim T_c$, the first term with the coherence factor $(1 + \Delta\Delta'/EE')$ gives the dominant contribution for the s_{++} -wave state. At $T = 0$, because of the thermal factor, the self energy becomes

$$\text{Im}\Sigma_{\mathbf{k}}^{\text{R}}(\omega) \approx -\frac{\pi V_{\text{eff}}^2}{8N^2} \sum_{\mathbf{k}'} \sum_{\mathbf{k}''} \left(1 - \frac{\Delta_{\mathbf{k}-\mathbf{k}'+\mathbf{k}''} \Delta_{\mathbf{k}''}}{E_{\mathbf{k}-\mathbf{k}'+\mathbf{k}''} E_{\mathbf{k}''}}\right) \delta(|\omega| - |E_{\mathbf{k}'} + E_{\mathbf{k}-\mathbf{k}'+\mathbf{k}''} + E_{\mathbf{k}''}|). \quad (24)$$

It is clear from the delta function that it equals 0 for $\omega < 3\Delta_{\text{min}}$.

Experimental studies on the iron pnictides such as ARPES⁵², point contact tunneling,⁵³ NQR³¹ and specific heat⁵⁴ have demonstrated that there are at least two different superconducting gaps, small gap Δ_{S} and large gap Δ_{L} . Multi-gap superconductivity has been seen in a number of systems including MgB₂ which is an s -wave superconductor with a T_c of 39 K.^{55,56} Based on these experiments, we set the small and large superconducting gaps as,

$$\begin{aligned} \Delta_{\alpha_1}^0 &= \Delta_{\alpha_2}^0 = \Delta_{\text{S}}, \\ \Delta_{\alpha_3}^0 &= \Delta_{\alpha_4}^0 = \pm\Delta_{\text{L}}, \\ (+: \text{ for } s_{++}, -: \text{ for } s_{\pm}). \end{aligned} \quad (25)$$

Hereafter, we employ these values as $2\Delta_{\text{L}}/T_c = 5$ and $\Delta_{\text{L}}/\Delta_{\text{S}} = 3$, which are approximately satisfied in various Co-doped 122 systems according to the specific heat measurements.⁵⁷

Figure 2 (a) shows the temperature dependence of $\tilde{\gamma} \equiv \gamma/V_{\text{eff}}^2 T_c^2$ on the s_{++} -wave superconducting state at various frequencies. The T dependence of $\tilde{\gamma}$ is small in the normal state ($T > T_c$), but $\tilde{\gamma}$ rapidly decreases with decreasing T in the superconducting state ($T < T_c$). Figure 2 (b) shows the ω dependence of $\tilde{\gamma}$. Two vertical dotted lines show the small and large superconducting gaps at zero temperature Δ_{S} and Δ_{L} , respectively. In the normal state, $\tilde{\gamma}$ is large due to the strong correlation. However, $\tilde{\gamma}$ is strongly suppressed in the superconducting state since the inelastic damping $\tilde{\gamma}$ is reduced as the superconducting gap opens. It is satisfied that $\gamma(\omega)|_{T=0} = 0$ for $\omega < 3\Delta_{\text{S}} = \Delta_{\text{L}}$.

Figures 3 (a) and (b) show the T and ω dependence of $\tilde{\gamma}$ on the s_{\pm} -wave superconducting state, respectively. As is the case in s_{++} , $\tilde{\gamma}$ is strongly suppressed for $T < T_c$. The obtained quasi-particle damping for s_{\pm} -wave state

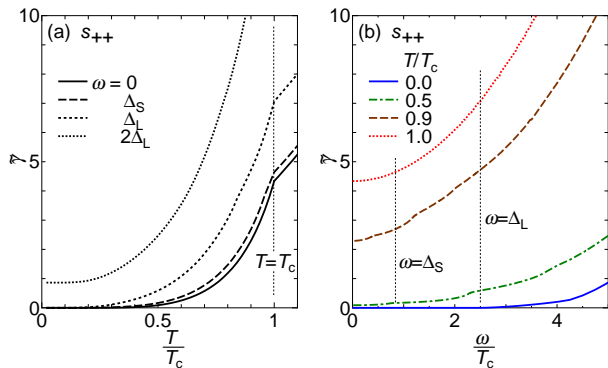


FIG. 2. (a) The temperature dependences of $\tilde{\gamma} \equiv \gamma/V_{\text{eff}}^2 T_c^2$ in the s_{++} -wave state with $2\Delta_L/T_c = 5$ and $\Delta_L/\Delta_S = 3$. Solid, dashed, short-dashed and dotted lines corresponds to $\omega = 0$, Δ_S , Δ_L and $2\Delta_L$, respectively. (b) ω dependences of $\tilde{\gamma}$ in the s_{++} -wave state for various T . Solid, dashed-dotted, dashed and dotted lines represent $T = 0$, $0.5T_c$, $0.9T_c$ and T_c , respectively. Vertical dotted lines show $\omega = \Delta_L$ and Δ_S .

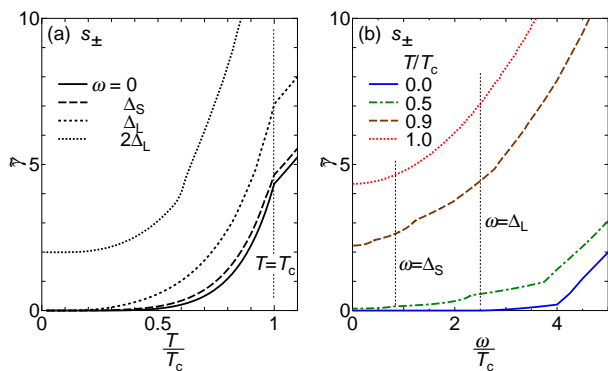


FIG. 3. (a) The T dependences of the $\tilde{\gamma}$ in the s_{\pm} -wave state with $2\Delta_L/T_c = 5$ and $\Delta_L/\Delta_S = 3$. (b) The ω dependences of the $\tilde{\gamma}$ in the s_{\pm} -wave state.

is similar to the s_{++} -wave state.

D. Quasiparticle Damping

In this subsection, we estimate the absolute value of the inelastic damping rate $\gamma(0)$ in the normal state, and thus yields the effective interaction V_{eff} , from the experimentally observed resistivity. From the Nakano-Kubo formula, the conductivity is given by,

$$\sigma = \frac{e^2}{4\pi c} \sum_{\alpha} \int_{\text{FS}\alpha} dk_{\parallel} \frac{|v_{\alpha, \mathbf{k}}|}{2\gamma(0)}, \quad (26)$$

where $\gamma(0)$ is the “unrenormalized” damping at zero energy, and $v_{\alpha, \mathbf{k}}$ is the Fermi velocity at \mathbf{k} on the α th Fermi surface. Here, we neglect the current vertex correction since it is not important for the diagonal conductivity⁵⁸. $\gamma(0)$ is derived from the theoretical relation between $\rho(T)$

TABLE I. T_c and other parameters of $\text{Ba}(\text{Fe}_{1-x}\text{Co}_x)_2\text{As}_2$ for various doping rate x .⁵⁹ $\gamma(0)$ is estimated by fitting the experimental data and V_{eff} is obtained by $\gamma(0)$ and $N(0) = 0.66 \text{ eV}^{-1}$. We note that we obtain $n = 1.0$ and $a = 0.63 \mu\Omega\text{cm/K}$ for $x = 0.08$ according to the measurement by Sefat *et al.*⁶¹ In this case, we obtain $V_{\text{eff}} = 19.9 \text{ eV}$. In this table, the units of ρ and a are $\mu\Omega\text{cm}$ and $\mu\Omega\text{cm/K}^n$, respectively.

Ba(Fe _{1-x} Co _x) ₂ As ₂ ⁵⁹				
x	0.08	0.12	0.14	0.20
T_c	24 K	17 K	11 K	-
$\rho(0)$	73	65	65	57
$\rho(T_c) - \rho(0)$	11.9	4.6	1.3	-
a	0.495	0.153	0.045	0.0011
n	1.0	1.2	1.4	2.0
$\gamma(0) _{T=T_c}$	0.0059 (= 69 K)	0.0023 (= 27 K)	0.00065 (= 7.5 K)	-
V_{eff}	17.7	15.5	12.7	4.3

and $\gamma(0)$,²⁷

$$\rho(T) - \rho(0) \approx \begin{cases} 0.0020\gamma(0) [\mu\Omega\text{cm}] & \text{for } c = 6 \text{ \AA} \\ 0.0028\gamma(0) [\mu\Omega\text{cm}] & \text{for } c = 8 \text{ \AA} \end{cases} \quad (27)$$

The interlayer spacing $c \approx 6 \text{ \AA}$ and $c \approx 8 \text{ \AA}$ are corresponding to the 122 and 1111 systems, respectively. On the other hand, we solve Eq. (21) as a normal state ($\text{Im}f^{0, \text{R}}(\omega) = 0$) and the inelastic damping rate $\gamma(0)$ is represented as

$$\gamma(0)|_{T=T_c} = \frac{\pi^3}{2} V_{\text{eff}}^2 N(0)^3 T_c^2. \quad (28)$$

Then, the effective interaction V_{eff} is derived by comparing Eq. (27) with Eq. (28).

In Table I, we show T_c and other parameters of $\text{Ba}(\text{Fe}_{1-x}\text{Co}_x)_2\text{As}_2$ for various doping rate x . The resistivity due to inelastic scattering, $\rho(T) - \rho(0)$, is estimated by fitting the experimental data below 150 K⁵⁹ with

$$\rho(T) = \rho(0) + aT^n. \quad (29)$$

where $\rho(0)$, a and n are free parameters. The obtained $\gamma = 69 \text{ K}$ for the optimally doped compound ($x = 0.08$) is larger than the transition temperature $T_c = 24 \text{ K}$. On the other hand, γ decreases rapidly by carrier doping, and $\gamma = 7.5 \text{ K}$ becomes smaller than $T_c = 11 \text{ K}$ for the over doped compound ($x = 0.14$). The estimated effective interaction V_{eff} is 17.7 eV for the optimally doped system, and 12.2 eV for the over doped system. V_{eff} is large as compared with the bare on-site Coulomb interaction $U = 2 \sim 3 \text{ eV}$ for $3d$ electrons on a Fe atom⁶⁰ because of the spin and charge Stoner enhancement that give large spin and orbital fluctuations.

III. RESULTS

In Figs. 4 and 5, we show the numerical results for T dependence of the nuclear spin relaxation rate for optimally and over doping states, respectively. According

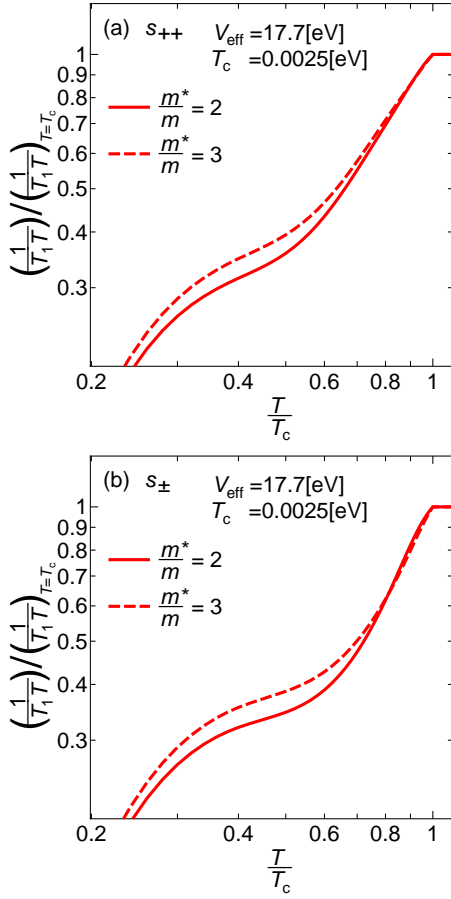


FIG. 4. The normalized nuclear relaxation rate $(1/T_1 T)/(1/T_1 T)|_{T=T_c}$ for optimally doping state ($T_c = 0.0025$ eV and $V_{\text{eff}} = 17.7$ eV) in the (a) s_{++} and (b) s_{\pm} -wave states as a function of reduced temperature T/T_c . Solid and dashed lines represent $m^*/m = 2$ and $m^*/m = 3$, respectively.

to Table I, effective potential $V_{\text{eff}} = 17.7$ eV for optimally doped systems and 12.7 eV for over doped systems. The mass enhancement factors are $m^*/m = 2 \sim 3$ for optimum doped systems and $m^*/m = 1 \sim 2$ for over doped system.^{46–50} Figures 4 (a) and (b) show $1/T_1 T$ in the s_{++} and s_{\pm} -wave states for optimally doping with $T_c = 0.0025$ eV and $V_{\text{eff}} = 17.7$ eV. Solid and dashed lines represent $m^*/m = 2$ and $m^*/m = 3$, respectively. In this case, the Hebel-Slichter coherence peak is suppressed even in both the s_{++} and s_{\pm} -wave states due to the strong inelastic quasi-particle damping $\gamma^*(0)|_{T_c} = 1.0 \sim 1.5T_c$.

Figures 5 (a) and (b) show $1/T_1 T$ for over-doped systems ($T_c = 0.0010$ eV and $V_{\text{eff}} = 12.7$ eV) in s_{++} and s_{\pm} -wave states, respectively. The coherence peak increase for smaller V_{eff} since γ is proportional to V_{eff}^2 . Since the coherence peak is suppressed by $\gamma^* = (m/m^*)\gamma$, it is more restored by larger m^*/m . Small coherence peak is recognized in over-doped s_{++} -wave state for $m^*/m = 2$. The insets of Figure 5 show $1/T_1 T$ for $T_c = 0.0005$ eV

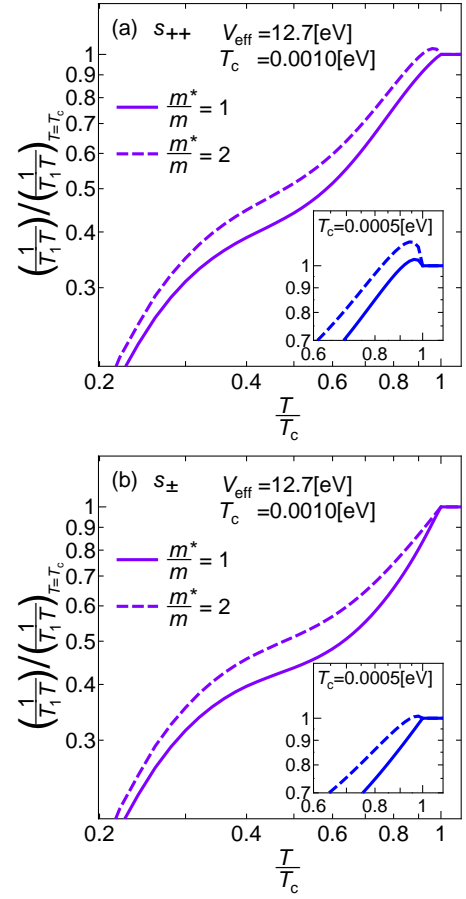


FIG. 5. The normalized nuclear relaxation rate $(1/T_1 T)/(1/T_1 T)|_{T=T_c}$ for over doping state ($T_c = 0.0010$ eV and $V_{\text{eff}} = 12.7$ eV) in the (a) s_{++} and (b) s_{\pm} -wave states as a function of reduced temperature T/T_c . Solid and dashed lines represent $m^*/m = 1$ and $m^*/m = 2$, respectively. $1/T_1 T$ for $T_c = 0.0005$ eV and $V_{\text{eff}} = 12.7$ eV are shown in the insets.

and $V_{\text{eff}} = 12.7$ eV. Since γ decreases in proportion to T_c^2 , small coherence peak appears in both s_{++} and s_{\pm} -wave states. These results indicate that the Hebel-Slichter coherence peak on $1/T_1 T$ might be observed for a sample with $T_c \sim 5$ K, as reported in Ref. 35.

We discuss the Hebel-Slichter peak in both s_{++} and s_{\pm} -wave states. We show the ω dependences of $X(\omega)$ (defined in Eq. (16)), $N^n(\omega)$ and $N^a(\omega)$ for over doped systems ($T_c = 0.0005$ eV, $V_{\text{eff}} = 12.7$ eV and $m^*/m = 2$) in Figs. 6 (a), (b) and (c), respectively. The integral of $X(\omega) = \pi(N^n(\omega)^2 + N^a(\omega)^2)(-\frac{\partial f}{\partial \omega})$ yields $1/T_1 T$. Two peaks in $X(\omega)$ at $T = 0.9T_c$ correspond two superconducting gaps Δ_S and $\pm\Delta_L$. These peaks yields the Hebel-Slichter peak in the inset of Fig. 5. For s_{\pm} -wave state, the sign of N^a reserves at $\omega \sim (\Delta_L + \Delta_S)/2$. Because of the relation $|N_{s_{++}}^a| \sim |N_{s_{\pm}}^a|$ in the present case $\Delta_L : \Delta_S = 3 : 1$, similar Hebel-Slichter peak appear in both superconducting states. On the other hand, for optimum doped systems ($T_c = 0.0025$ eV, $V_{\text{eff}} = 17.7$ eV

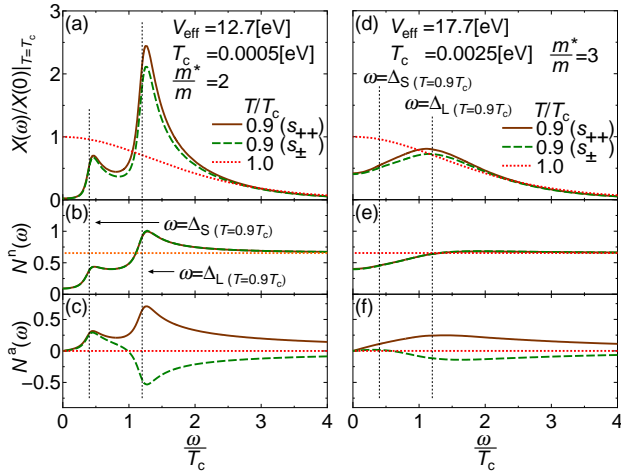


FIG. 6. (a) The ω dependence of $X(\omega)/X(0)|_{T=T_c}$ in over doped systems for $T_c = 0.0005$ eV, $V_{\text{eff}} = 12.7$ eV and $m^*/m = 2$. Solid, dashed and dotted lines represent s_{++} and s_{\pm} -wave states ($T = 0.9T_c$) and normal state ($T = T_c$), respectively. (b) $N^n(\omega) \equiv -\frac{1}{\pi}\text{Im}f^R(\omega)$. (c) $N^a(\omega) \equiv -\frac{1}{\pi}\text{Im}f^R(\omega)$. (d)-(f) $X(\omega)$, N^n and N^a in optimum doped systems for $T_c = 0.0025$, $V_{\text{eff}} = 17.7$ eV and $m^*/m = 3$. Vertical dotted lines show $\omega = \Delta_S$ and Δ_L at $T = 0.9T_c$.

and $m^*/m = 3$), these peaks in $X(\omega)$ are suppressed due to strong γ at $T = 0.9T_c$ as shown in Figs. 6 (d) - (f). In this case, the Hebel-Slichter peak disappears as shown in Fig. 4.

IV. SUMMARY AND DISCUSSION

To summarize, we investigate the nuclear magnetic relaxation rate $1/T_1T$, especially paying attention to the presence of the coherence peak for both s_{++} and s_{\pm} -wave states base on the five orbital model. The inelastic quasi-particle damping rate γ at T_c is estimated from the experimental results of the resistivity, and T - and ω -dependences of γ are calculated using the second order perturbation theory.

Using parameters for optimally doped systems, the Hebel-Slichter coherence peak on $1/T_1T$ is suppressed due to the strong $\gamma^*(0)|_{T_c} \sim T_c$ even in the s_{++} -wave state for $T \geq 10$ K. This result is consistent with previous strong coupling theories.^{36,37} On the other hand, the relation $\gamma^*(0)|_{T_c} \ll T_c$ is expected in heavily over doped systems with $T_c \sim 5$ K: In this case, coherence peak may appear for both pairing states. Note that the tiny coherence peak in Fig. 5 (b) in the s_{\pm} -wave state grows comparable to that in 5 (a) in the s_{++} -wave state by halving the value of $\gamma^*(0)$. Thus, the condition for the appearance of coherence peak is similar for both s_{++} and s_{\pm} -wave states, so it is difficult to discriminate between these pairing states from the present NMR experimental data.

In Refs. 43 and 44, the authors measured $1/T_1$

and discussed the effect of γ on the coherence peak. They assumed the functional form $\gamma(\omega) = \gamma(0)|_{T=T_c} \exp[A(T/T_c - 1)]$ (ω dependence was neglected), and chose parameters $A = 5$ and $\gamma(0)|_{T_c} = 3T_c$, and found that the coherence peak disappears even in the s_{++} -wave state. The large damping $\gamma(0)|_{T_c} = 3T_c$ is comparable to our estimation ($1.0 \sim 1.5T_c$) for optimum doping systems, so their analysis is consistent with the present study.

In this paper, we discussed only Co-doped Ba122 systems, since reliable resistivity data in single crystals are available. The coherence peak is also absent in LiFeAs ($c = 6.36$ Å, $T_c = 17$ K)⁶². In this compound, the resistivity is fitted as $\rho(T) = \rho_0 + aT^2$ and $a = 0.022 \mu\Omega\text{cm}/\text{K}^2$ in Ref. 63. Then, the obtained effective potential is $V_{\text{eff}} = 15.9$ meV, which is comparable to the value of optimally doped Ba(Fe,Co)₂As₂ (17.5 meV). Therefore, if we assume the gap structure given by ARPES measurements ($\Delta_L \sim \Delta_S \sim 3$ meV)^{64,65} the coherence peak disappears even for the s_{++} -wave state. However, since the size of each hole-pocket in LiFeAs^{64,65} are different from that in Ba(Fe,Co)₂As₂, more realistic tight-binding model for LiFeAs would be required for a quantitative analysis.

In LaFeAsO_{1-x}F_x, we cannot estimate γ quantitatively because of the lack of resistivity data in single crystals. For a qualitative analysis, however, we can roughly estimate the single crystal resistivity of LaFeAsO_{1-x}F_x from the poly crystal resistivity in Ref. 66 by multiplying the factor 1/3, as discussed in Ref. 11. Using this method, we can fit them by using $\rho(T) = \rho(0) + aT^2$ and obtain $\gamma(0)|_{T_c} \sim 0.0023$ eV and $V_{\text{eff}} \sim 10.2$ eV for LaFeAsO_{0.89}F_{0.11} ($T_c = 26$ K). Using these parameters, the Hebel-Slichter coherence peak for optimally doped La1111 systems are also suppressed in both s_{++} and s_{\pm} -wave states.

In both LiFeAs and La1111, conventional Fermi liquid resistivity ($\rho \propto T^2$) is observed. This fact would be consistent with the small spin fluctuations in these compounds. However, γ at T_c is large enough to suppress the coherence peak. Thus, both compounds are strongly correlated Fermi liquids due to relatively local fluctuations. In Sm1111 and Nd1111 ($T_c > 50$ K), the T -linear-type behavior of resistivity is observed, indicating the enhancement of fluctuations as As₄ tetrahedron approaches to a regular tetrahedron.¹⁸

We stress that the inelastic scattering γ also plays important roles in the neutron scattering spectrum: In neutron magnetic scattering measurements, broad "resonance-like" peak structure is observed in many FeAs superconductors below T_c , and this fact had been frequently ascribed to the resonance due to the gap sign change. However, the "resonance condition" is not surely confirmed since it is difficult to determine the gap size accurately. The resonance condition in FeAs superconductor is $\omega_{\text{res}} < \Delta_L + \Delta_S$, where ω_{res} denotes the peak energy of neutron scattering. In the following, we write down the experimental values of ω_{res} , Δ_L and Δ_S .

(A) BaFe_{1.85}Co_{0.15}As₂: $\omega_{\text{res}} = 10$ meV by neutron.⁶⁷

* Specific heat:⁵⁴

$$\Delta_L = 5 \text{ meV}, \Delta_S = 2 \text{ meV}; \Delta_L + \Delta_S = 7 \text{ meV}$$

* Penetration depth:⁶⁸

$$\Delta_L = 6.1 \text{ meV}, \Delta_S = 2.3 \text{ meV}; \Delta_L + \Delta_S = 8.4 \text{ meV}$$

* ARPES:⁶⁹

$$\Delta_L = 6.6 \text{ meV}, \Delta_S = 5 \text{ meV}; \Delta_L + \Delta_S = 11.6 \text{ meV}$$

(B) FeTe_{0.6}Se_{0.4}: $\omega_{\text{res}} = 7$ meV by neutron.⁷⁰

* ARPES:⁷¹

$$\Delta_L = 4.2 \text{ meV}, \Delta_S = 2.5 \text{ meV}; \Delta_L + \Delta_S = 6.7 \text{ meV}.$$

In case (A), the resonance condition $\omega_{\text{res}} < \Delta_L + \Delta_S$ is satisfied only by ARPES data. In case (B), although ARPES tends to report larger gap size in FeAs superconductors, the resonance condition is still unclear.

Theoretically, we have revealed that broad hump structure at $\omega \sim \Delta_L + \Delta_S$ can appear even in the s_{++} -wave state, not due to the resonance but due to strong suppression of inelastic quasi-particle scattering rate $\gamma(\omega)$ for $|\omega| < 3\Delta$ ("dissipation-less mechanism"^{26,27}). Thus, both the absence of the coherence peak in $1/T_1T$ as well

as the hump structure in the neutron scattering spectrum are explained by the same many-body effect — inelastic quasi-particle scattering — using similar inelastic scattering rate $\gamma(0)$ evaluated from the resistivity.

Finally, we comment that large inelastic scattering γ at T_c in Fe based superconductors also works as the depairing effect. In the random-phase-approximation (RPA), in which the depairing effect due to inelastic scattering is neglected, the obtained T_c is about 200 K.^{5,16} However, in the fluctuation-exchange (FLEX) approximation, the obtained T_c is strongly suppressed (below 50 K) due to the the depairing effect (self-energy correction).¹⁷

ACKNOWLEDGMENTS

We are grateful to M. Sato and Y. Kobayashi for useful comments and discussions. This study has been supported by Grants-in-Aid for Scientific Research from MEXT of Japan, and by JST, TRIP.

-
- ¹ Y. Kamihara, T. Watanabe, M. Hirano, and H. Hosono, *J. Am. Chem. Soc.* **130**, 3296 (2008).
- ² K. Hashimoto, T. Shibauchi, T. Kato, K. Ikada, R. Okazaki, H. Shishido, M. Ishikado, H. Kito, A. Iyo, H. Eisaki, S. Shamoto, and Y. Matsuda, *Phys. Rev. Lett.* **102**, 017002 (2009).
- ³ H. Ding, P. Richard, K. Nakayama, K. Sugawara, T. Arakane, Y. Sekiba, A. Takayama, S. Souma, T. Sato, T. Takahashi, Z. Wang, X. Dai, Z. Fang, G. F. Chen, J. L. Luo, and N. L. Wang, *Europhys. Lett.* **83**, 47001 (2008).
- ⁴ T. Kondo, A. F. Santander-Syro, O. Copie, C. Liu, M. E. Tillman, E. D. Mun, J. Schmalian, S. L. Bud'ko, M. A. Tanatar, P. C. Canfield, and A. Kaminski, *Phys. Rev. Lett.* **101**, 147003 (2008).
- ⁵ K. Kuroki, S. Onari, R. Arita, H. Usui, Y. Tanaka, H. Kontani, and H. Aoki, *Phys. Rev. Lett.* **101**, 087004 (2008).
- ⁶ I. I. Mazin, D. J. Singh, M. D. Johannes, and M. H. Du, *Phys. Rev. Lett.* **101**, 057003 (2008).
- ⁷ A. V. Chubukov, D. V. Efremov, and I. Eremin, *Phys. Rev. B* **78**, 134512 (2008).
- ⁸ P. J. Hirschfeld, M. M. Korshunov, and I. I. Mazin, *Rep. Prog. Phys.* **74**, 124508 (2011).
- ⁹ V. Cvetkovic and Z. Tesanovic, *Europhys. Lett.* **85**, 37002 (2009).
- ¹⁰ T. Hanaguri, S. Niitaka, K. Kuroki, and H. Takagi, *Science* **328**, 474 (2010).
- ¹¹ A. Kawabata, S. C. Lee, T. Moyoshi, Y. Kobayashi, and M. Sato, *J. Phys. Soc. Jpn.* **77**, 103704 (2008).
- ¹² Y. Nakajima, T. Taen, Y. Tsuchiya, T. Tamegai, H. Kitamura, and T. Murakami, *Phys. Rev. B* **82**, 220504 (2010).
- ¹³ J. Li, Y. Guo, S. Zhang, S. Yu, Y. Tsujimoto, H. Kontani, K. Yamaura, and E. Takayama-Muromachi, *Phys. Rev. B* **84**, 020513 (2011).
- ¹⁴ K. Kirshenbaum, S. R. Saha, S. Ziemak, T. Drye, and J. Paglione, arXiv:1203.5114.
- ¹⁵ S. Onari and H. Kontani, *Phys. Rev. Lett.* **103**, 177001 (2009).
- ¹⁶ H. Kontani and S. Onari, *Phys. Rev. Lett.* **104**, 157001 (2010).
- ¹⁷ S. Onari and H. Kontani, *Phys. Rev. B* **85**, 134507 (2012).
- ¹⁸ T. Saito, S. Onari, and H. Kontani, *Phys. Rev. B* **82**, 144510 (2010).
- ¹⁹ H. Kontani, T. Saito, and S. Onari, *Phys. Rev. B* **84**, 024528 (2011).
- ²⁰ S. Onari and H. Kontani, arXiv:1203.2874.
- ²¹ H. Kontani, Y. Inoue, T. Saito, Y. Yamakawa, and S. Onari, *Solid State Commun.* **152**, 718 (2012).
- ²² R. M. Fernandes, L. H. VanBebber, S. Bhattacharya, P. Chandra, V. Keppens, D. Mandrus, M. A. McGuire, B. C. Sales, A. S. Sefat, and J. Schmalian, *Phys. Rev. Lett.* **105**, 157003 (2010).
- ²³ T. Goto, R. Kurihara, K. Araki, K. Mitsumoto, M. Akatsu, Y. Nemoto, S. Tatematsu, and M. Sato, *J. Phys. Soc. Jpn.* **80**, 073702 (2011).
- ²⁴ M. Yoshizawa, D. Kimura, T. Chiba, S. Simayi, Y. Nakanishi, K. Kihou, C. Lee, A. Iyo, H. Eisaki, M. Nakajima, and S. Uchida, *J. Phys. Soc. Jpn.* **81**, 024604 (2012).
- ²⁵ J. L. Niedziela, D. Parshall, K. A. Lokshin, A. S. Sefat, A. Alatas, and T. Egami, *Phys. Rev. B* **84**, 224305 (2011).
- ²⁶ S. Onari, H. Kontani, and M. Sato, *Phys. Rev. B* **81**, 060504 (2010).
- ²⁷ S. Onari and H. Kontani, *Phys. Rev. B* **84**, 144518 (2011).
- ²⁸ L. C. Hebel and C. P. Slichter, *Phys. Rev.* **113**, 1504 (1959).
- ²⁹ Y. Nakai, K. Ishida, Y. Kamihara, M. Hirano, and H. Hosono, *J. Phys. Soc. Jpn.* **77**, 073701 (2008).
- ³⁰ H. Grafe, D. Paar, G. Lang, N. J. Curro, G. Behr, J. Werner, J. Hamann-Borrero, C. Hess, N. Leps, R. Klingeler, and B. Büchner, *Phys. Rev. Lett.* **101**, 047003 (2008).

- ³¹ S. Kawasaki, K. Shimada, G. F. Chen, J. L. Luo, N. L. Wang, and G.-q. Zheng, *Phys. Rev. B* **78**, 220506 (2008).
- ³² F. Ning, K. Ahilan, T. Imai, A. S. Sefat, R. Jin, M. A. McGuire, B. C. Sales, and D. Mandrus, *J. Phys. Soc. Jpn.* **78**, 013711 (2009).
- ³³ M. Yashima, H. Nishimura, H. Mukuda, Y. Kitaoka, K. Miyazawa, P. M. Shirage, K. Kihou, H. Kito, H. Eisaki, and A. Iyo, *J. Phys. Soc. Jpn.* **78**, 103702 (2009).
- ³⁴ Y. Kobayashi, A. Kawabata, S. C. Lee, T. Moyoshi, and M. Sato, *J. Phys. Soc. Jpn.* **78**, 073704 (2009).
- ³⁵ H. Mukuda, M. Nitta, M. Yashima, Y. Kitaoka, P. M. Shirage, H. Eisaki, and A. Iyo, *J. Phys. Soc. Jpn.* **79**, 113701 (2010).
- ³⁶ R. Akis and J. Carbotte, *Solid State Commun.* **78**, 393 (1991).
- ³⁷ S. Fujimoto, *J. Phys. Soc. Jpn.* **61**, 765 (1992).
- ³⁸ T. Kohara, T. Oda, K. Ueda, Y. Yamada, A. Mahajan, K. Elankumar, Z. Hossian, L. C. Gupta, R. Nagarajan, R. Vijayaraghavan, and C. Mazumdar, *Phys. Rev. B* **51**, 3985 (1995).
- ³⁹ Y. Kishimoto, T. Ohno, and T. Kanashiro, *J. Phys. Soc. Jpn.* **64**, 1275 (1995).
- ⁴⁰ Y. Bang and H. Choi, *Phys. Rev. B* **78**, 134523 (2008).
- ⁴¹ D. Parker, O. V. Dolgov, M. M. Korshunov, A. A. Golubov, and I. I. Mazin, *Phys. Rev. B* **78**, 134524 (2008).
- ⁴² Y. Senga and H. Kontani, *New J. Phys.* **11**, 035005 (2009).
- ⁴³ M. Sato, Y. Kobayashi, S. C. Lee, H. Takahashi, E. Satomi, and Y. Miura, *J. Phys. Soc. Jpn.* **79**, 014710 (2010).
- ⁴⁴ M. Sato and Y. Kobayashi, *Solid State Commun.* **152**, 688 (2012).
- ⁴⁵ P. B. Allen and B. Mitrović, *Theory of Superconducting Tc*, (*Solid State Physics* **37**: 1-92, 1982).
- ⁴⁶ S. E. Sebastian, J. Gillett, N. Harrison, P. H. C. Lau, D. J. Singh, C. H. Mielke, and G. G. Lonzarich, *J. Phys.: Condens. Matter* **20**, 422203 (2008).
- ⁴⁷ J. G. Analytis, C. M. J. Andrew, A. I. Coldea, A. McCollam, J. Chu, R. D. McDonald, I. R. Fisher, and A. Carrington, *Phys. Rev. Lett.* **103**, 076401 (2009).
- ⁴⁸ H. Shishido, A. F. Bangura, A. I. Coldea, S. Tonegawa, K. Hashimoto, S. Kasahara, P. M. C. Rourke, H. Ikeda, T. Terashima, R. Settai, Y. O-nuki, D. Vignolles, C. Proust, B. Vignolle, A. McCollam, Y. Matsuda, T. Shibauchi, and A. Carrington, *Phys. Rev. Lett.* **104**, 057008 (2010).
- ⁴⁹ M. M. Qazilbash, J. J. Hamlin, R. E. Baumbach, L. Zhang, D. J. Singh, M. B. Maple, and D. N. Basov, *Nat. Phys.* **5**, 647 (2009).
- ⁵⁰ T. Okuda, W. Hirata, A. Takemori, S. Suzuki, S. Saijo, S. Miyasaka, and S. Tajima, *J. Phys. Soc. Jpn.* **80**, 044704 (2011).
- ⁵¹ H. A. Weldon, *Phys. Rev. D* **28**, 2007 (1983).
- ⁵² P. Richard, T. Sato, K. Nakayama, T. Takahashi, and H. Ding, *Rep. Prog. Phys.* **74**, 124512 (2011).
- ⁵³ P. Samuely, P. Szabó, Z. Pribulová, M. E. Tillman, S. L. Bud'ko, and P. C. Canfield, *Superc. Sci. Technol.* **22**, 014003 (2009).
- ⁵⁴ F. Hardy, P. Burger, T. Wolf, R. A. Fisher, P. Schweiss, P. Adelman, R. Heid, R. Fromknecht, R. Eder, D. Ernst, H. v. Löhneysen, and C. Meingast, *Europhys. Lett.* **91**, 47008 (2010).
- ⁵⁵ J. Nagamatsu, N. Nakagawa, T. Muranaka, Y. Zenitani, and J. Akimitsu, *Nature* **410**, 63 (2001).
- ⁵⁶ A. Y. Liu, I. I. Mazin, and J. Kortus, *Phys. Rev. Lett.* **87**, 087005 (2001).
- ⁵⁷ D. C. Johnston, *Adv. Phys.* **59**, 803 (2010).
- ⁵⁸ H. Kontani, *Rep. Prog. Phys.* **71**, 026501 (2008).
- ⁵⁹ F. Rullier-Albenque, D. Colson, A. Forget, and H. Alloul, *Phys. Rev. Lett.* **103**, 057001 (2009).
- ⁶⁰ T. Miyake, K. Nakamura, R. Arita, and M. Imada, *J. Phys. Soc. Jpn.* **79**, 044705 (2010).
- ⁶¹ A. S. Sefat, D. J. Singh, R. Jin, M. A. McGuire, B. C. Sales, F. Ronning, and D. Mandrus, *Physica C* **469**, 350 (2009).
- ⁶² Z. Li, Y. Ooe, X.-C. Wang, Q.-Q. Liu, C.-Q. Jin, M. Ichioka, and G. Zheng, *J. Phys. Soc. Jpn.* **79**, 083702 (2010).
- ⁶³ O. Heyer, T. Lorenz, V. B. Zabolotnyy, D. V. Evtushinsky, S. V. Borisenko, I. Morozov, L. Harnagea, S. Wurmehl, C. Hess, and B. Buchner, *Phys. Rev. B* **84**, 064512 (2011).
- ⁶⁴ K. Umezawa, Y. Li, H. Miao, K. Nakayama, Z.-H. Liu, P. Richard, T. Sato, J. B. He, D.-M. Wang, G. F. Chen, H. Ding, T. Takahashi, and S.-C. Wang, *Phys. Rev. Lett.* **108**, 037002 (2012).
- ⁶⁵ S. V. Borisenko, V. B. Zabolotnyy, A. A. Kordyuk, D. V. Evtushinsky, T. K. Kim, I. V. Morozov, R. Follath, and B. Buchner, *Symmetry* **4**, 251 (2012).
- ⁶⁶ A. S. Sefat, M. A. McGuire, B. C. Sales, R. Jin, J. Y. Howe, and D. Mandrus, *Phys. Rev. B* **77**, 174503 (2008).
- ⁶⁷ D. S. Inosov, J. T. Park, P. Bourges, D. L. Sun, Y. Sidis, A. Schneidewind, K. Hradil, D. Haug, C. T. Lin, B. Keimer, and V. Hinkov, *Nature Phys.* **6**, 178 (2010).
- ⁶⁸ L. Luan, O. M. Auslaender, T. M. Lippman, C. W. Hicks, B. Kalisky, J.-H. Chu, J. G. Analytis, I. R. Fisher, J. R. Kirtley, and K. A. Moler, *Phys. Rev. B* **81**, 100501 (2010).
- ⁶⁹ K. Terashima, Y. Sekiba, J. H. Bowen, K. Nakayama, T. Kawahara, T. Sato, P. Richard, Y.-M. Xu, L. J. Li, G. H. Cao, Z.-A. Xu, H. Ding, and T. Takahashi, *Proc. Natl. Acad. Sci.* **106**, 7330 (2009).
- ⁷⁰ L. W. Harriger, O. J. Lipscombe, C. Zhang, H. Luo, M. Wang, K. Marty, M. D. Lumsden, and P. Dai, *Phys. Rev. B* **85**, 054511 (2012).
- ⁷¹ H. Miao, P. Richard, Y. Tanaka, K. Nakayama, T. Qian, K. Umezawa, T. Sato, Y.-M. Xu, Y. B. Shi, N. Xu, X.-P. Wang, P. Zhang, H.-B. Yang, Z.-J. Xu, J. S. Wen, G.-D. Gu, X. Dai, J.-P. Hu, T. Takahashi, and H. Ding, *Phys. Rev. B* **85**, 094506 (2012).